metals

MDPI

Article

Leaching Behavior of Lithium-Bearing Bauxite with High-Temperature Bayer Digestion Process in K_2O-Al_2O_3-H_2O System

Dongzhan Han [1,2], Zhihong Peng [1,*], Erwei Song [2] and Leiting Shen [1]

[1] School of Metallurgy and Environment, Central South University, Changsha 410083, China; hdzhan@csu.edu.cn (D.H.); shenleiting@csu.edu.cn (L.S.)
[2] Zhengzhou Non-Ferrous Metals Research Institute Co. Ltd. of CHALCO, Zhengzhou 450041, China; zyy_sew@rilm.com.cn
* Correspondence: pengzh@csu.edu.cn

Abstract: Lithium is one of the secondary mineral elements occurring in bauxite. The behavior of lithium-bearing bauxite in the digestion process was investigated, and the effect of digestion conditions on the extraction rates of lithium was studied. The results demonstrate that the mass ratio of the added CaO to bauxite, the KOH concentration, and the digestion temperature had a significant effect on the lithium extraction efficiency. An L9(3^4) orthogonal experiment demonstrated that the order of each factor for lithium extraction from primary to secondary is lime dosage, caustic concentration, and reaction temperature. Under the optimal conditions (t = 60 min, T = 260 °C, $\rho(K_2O)$ = 280 g/L, and 16% lime dosage), the leaching efficiencies of lithium and alumina are 85.6% and 80.09%, respectively, with about 15% of lithium entering into red mud. The findings of this study maybe useful for controlling lithium content in alumina products and lithium recovery from the Bayer process.

Keywords: lithium-bearing bauxite; digestion; K_2O-Al_2O_3-H_2O system

Citation: Han, D.; Peng, Z.; Song, E.; Shen, L. Leaching Behavior of Lithium-Bearing Bauxite withHigh-Temperature Bayer Digestion Process in K_2O-Al_2O_3-H_2O System. *Metals* **2021**, *11*, 1148. https://doi.org/10.3390/met11071148

Academic Editors: Antoni Roca and Jean-François Blais

Received: 24 May 2021
Accepted: 12 July 2021
Published: 20 July 2021

1. Introduction

Lithium is one of the secondary mineral elements occurring in bauxite, where lithium content can reach up to 0.3% (as Li_2O) [1–3].During the digestion process, lithium in bauxite is extracted into Bayer liquor, and in the following seed precipitation process, it co-precipitates with alumina hydroxide (ATH), resulting in high lithium content in alumina and, consequently, raising lithium impurity content of alumina products in China, which seriously impacts product quality and the competitiveness of refineries. Moreover, lithium impurity accumulation in the aluminum cell during electrolysis [4,5] leads to excessive (4–8%) LiF content in molten electrolytes and brings a series of serious problems to the electrolytic process, such as worsening stability of electrolytic cells and the difficulty of production operation, which affect electrolytic cell stability and the technical-economic index [6–9].

Lithium is a common impurity in the Bayer process using Chinese bauxite. A series of studies have been conducted, such as the equilibrium concentration and existence form of lithium in liquor and processes related to its removal and purification. Huang et al. [5] found that the equilibrium concentration of lithium ions in the sodium aluminate solution with pure substance can be increased with elevated temperature, caustic concentration, and declined alumina concentration. During crystal seed decomposition [10], lithium ions can promote secondary nucleation, increasing the content of fine particles and changing the crystal morphology of aluminum hydroxide. Restidge et al. [11] found that lithium ions can promote the precipitation and growth of ATH in extremely dilute liquor, some even co-precipitating with ATH. Vanstraten et al. [12] found that lithium exists in the form

of lithium-ion in dilute liquor and can react with $Al(OH)_4^-$ to form $LiA1_2(OH)_7{\cdot}2H_2O$. Xu et al. [13] found that a H_2TiO_3 ion sieve has a good purification effect on lithium ions in Bayer liquor, which can remove lithium from liquor (56 mg/L to less than 1.0 mg/L). When Tang Wen-qi et al. [14] synthesized highly active ATH to remove lithium from liquor with appropriate reaction conditions, the removal rate of lithium could reach 80.04%. The removal mechanism of lithium in liquor was also studied. The illite content of bauxite in Henan and Guizhou is high [15]. In the digestion process, potassium of illite is extracted into liquor, resulting in a potassium oxide content of liquor above 100 g/L. Potassium impurity in the Bayer liquor can contribute to elevate SiO_2 equilibrium concentrations, namely inhibiting the conversion of desilication products from natriuretic to calcite during the process of slurry preheat and digestion [16,17]. Moreover, as potassium aluminate is different from sodium aluminate solution, the lithium reactive behavior of the two leaching mediums also differs. Although the equilibrium concentration of lithium in sodium aluminate [5] is increased with elevated temperature and caustic concentration, few detailed investigations and evaluations of lithium-bearing bauxite in the high-temperature Bayer digestion process have been reported, especially in K_2O-Al_2O_3-H_2O systems.

In this study, the leaching behavior of lithium-bearing diaspore at high temperatures was studied, and the results of investigation on this process are presented. The findings of this study maybe useful for controlling lithium content in alumina products and lithium recovery from the Bayer process.

2. Experimental Section

2.1. Materials

The lithium-bearing diasporic bauxites used in this study were obtained from Henan province. All the bauxite was crushed and ground to a 250 μm (>75 wt%) particle size distribution as shown in Table 1 and then sampled for compositional analysis and phase identification. Table 2 shows that the main chemical components in the bauxite sample are Al_2O_3 and SiO_2 at 64.92% and 12.95%, respectively, followed by Fe_2O_3, TiO_2 (2.94% and 2.48%, respectively), and lithium (0.14%, as Li_2O). The mineral phase compositions are presented in Table 3, together with the X-ray diffraction result. Figure 1 illustrates that the available alumina in this bauxite occurs as diaspore. The main silicon-bearing minerals are kaolinite, illite, and quartz (24.5%, 7%, and 0.5 wt%, respectively), while the main iron-bearing mineral is hematite, at about 1.7 wt%. The main titanium-bearing minerals are anatase and rutile (2.0 wt% and 0.5 wt%, respectively), and the main lithium-bearing mineral is cookeite.

Table 1. Particle size distribution of lithium-bearing bauxite (%).

+250 μm	150–250 μm	90–150 μm	45–90 μm	–45 μm
22.3	28.4	11.1	7.60	30.6

Table 2. Chemical composition of lithium-bearing bauxite (%).

Al	Si	Fe	Ti	K	Na	Ca	Mg	Li	A/S
34.4	6.04	2.06	1.49	0.61	0.032	0.12	0.13	0.07	5.01

Table 3. Mineral phase composition of lithium-bearing bauxite (%).

Diaspore	Kaolinite	Hematite	Illite	Quartz	Anatase	Rutile
62.5	24.5	1.7	7.0	0.5	2.0	0.5

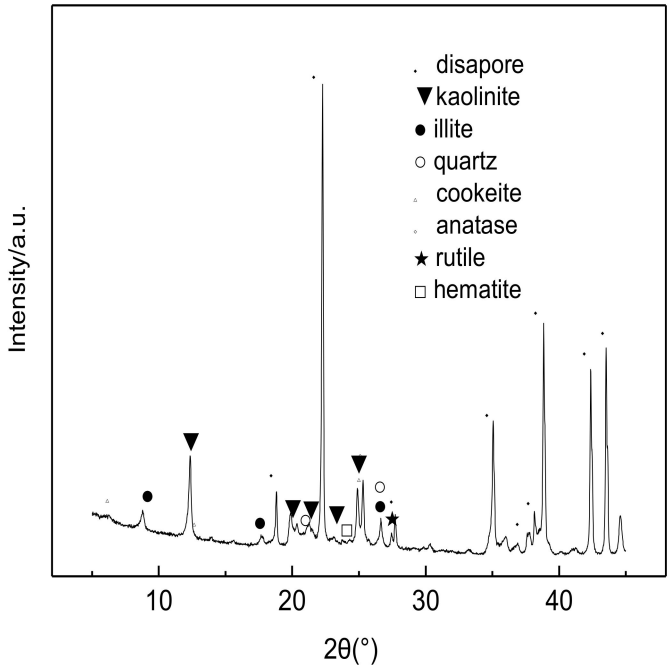

Figure 1. XRD pattern of lithium-bearing bauxite.

Bayer liquor, with 254 gL^{-1} K_2O and 144.6 gL^{-1} Al_2O_3, was prepared by dissolving alumina hydroxide and potassium hydroxide in boiling water.

2.2. Experimental Procedure

Digestion experiments were conducted using steel bombs heated in molten salt. After a designated duration, the bombs were removed from the molten salt cell and immediately placed in cold water to cool. Subsequently, solid-liquid separation was conducted by vacuum filtration, and the chemical composition of the dissolved liquid was analyzed, while solids were washed with deionized hot water and then dried at 100 °C for 6 h before analysis.

2.3. Characterization

Based on the A/S (mole ratio of alumina to silica) in bauxite and red mud, the digestion efficiency of alumina was calculated with Equation (1).

$$\eta_A = \frac{(A/S)_b - (A/S)_r}{(A/S)_b} \times 100\% \quad (1)$$

where η_A is the digestion efficiency of alumina, and $(A/S)_b$ and $(A/S)_r$ are the mole ratios of alumina to silica in bauxite and red mud, respectively.

The lithium extraction efficiency was calculated based on the lithium content and mass of red mud with Equation (2).

$$\eta_L = \left(1 - \frac{m_1 \times w_1}{m_2 \times w_2}\right) \times 100\% \quad (2)$$

where η_L is lithium extraction efficiency; m_1 and m_2 represent the masses of bauxite and red mud, respectively; and w_1, w_2 represent the lithium contents in bauxite and red mud, respectively.

The chemical composition of bauxite was analyzed by X-ray fluorescence spectrometry (XRF). The mineral phases were identified by X-ray diffraction, TTR III, Cu Kα radiation (Rigaku, Tokyo, Japan). Semi quantitative analysis of the phase content was carried out using the relative intensity ratio (RIR) method [18,19]. The lithium concentration in the

sodium aluminate solution was analyzed with an inductively coupled plasma atomic emission spectrometer (ICP-OES, Thermo Scientific ICAP 7200 Radial, Thermo Fisher Scientific, Waltham, MA, USA).

3. Results and Discussion

3.1. The Effects of Lime Dosage on Lithium and Alumina Extraction Efficiency

The digestion procedures were conducted at a caustic content of 254 g/L and at 260 °C for 60 min with different lime dosages to explore the effects of lime addition on the alumina and lithium extraction rates. The results are shown in Figure 2, which demonstrates that the addition of CaO had a significant effect on the lithium extraction efficiency. As the lime dosage increased from 0% to 8%, lithium extraction efficiency increased from 59.05% to 80%. When the lime dosage increased to 16%, the leaching efficiency gradually reached the maximum value of 89.81%. As the lime dosage exceeded 16%, the lithium extraction efficiency declined with an increase in lime dosage. It is therefore speculated that the Li^+ ion may be absorbed by the formed hydrogarnet (Figure 3). Lime can promote the leaching of alumina from bauxite. The lime dosage was greater than 8%, the alumina extraction efficiency declined, and excess lime and aluminum oxide formed hydrogarnet, leading to the decrease in the extraction rate of alumina and excess lime and aluminum oxide formed hydrogarnet, leading to the decrease in the extraction rate of alumina.

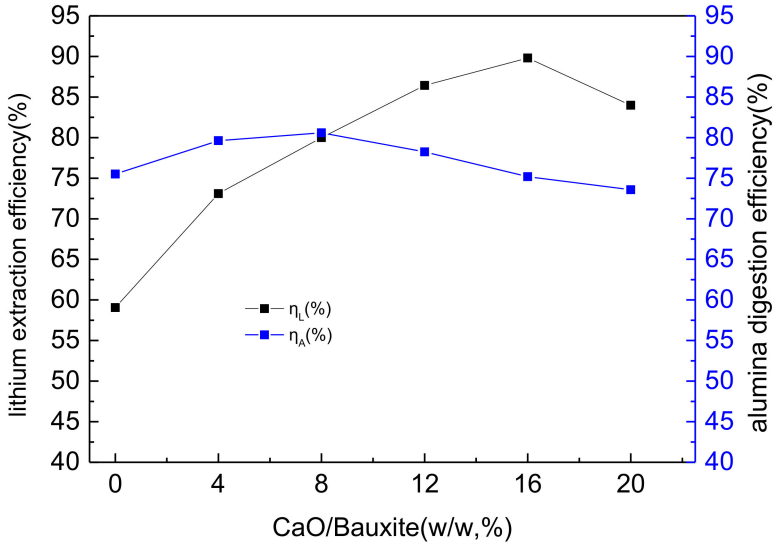

Figure 2. Effect of lime addition on lithium digestion behavior of bauxite (conditions: $\rho(K_2O)$ = 254 g/L, T = 265 °C, t = 1 h).

Figure 3 shows that no characteristic peak of lithium chlorite was observed, indicating lithium chlorite and KOH react completely with lime. $K_{1.33}(H_2O)_{0.33}Ti_4O_{8.33}(OH)_{0.67}$ was generated during titanium-containing mineral reactionswith KOH and without the addition of lime, which formed a film on the surface of the diaspore and prevented further reaction between leach solution and the diaspore; therefore, alumina digestion efficiency was low. With the addition of lime, the $K_{1.33}(H_2O)_{0.33}Ti_4O_{8.33}(OH)_{0.67}$ in the leach residue that inhibits dissolution disappeared, therefore promoting the decomposition of the diaspore [20–22]. Similar to the alumina leaching of diaspore digestion, the addition of CaO in this study also greatly promoted the decomposition of cookeite.

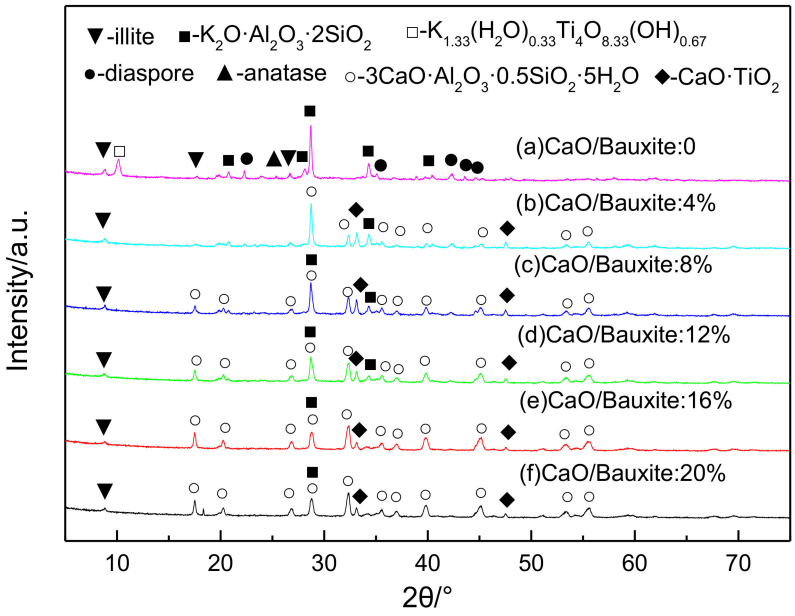

Figure 3. XRD patterns of red mud with different mass ratios of CaO/bauxite (conditions: $\rho(K_2O)$ = 254 g/L, T = 265 °C, t = 1 h).

3.2. The Effects of Caustic Concentration on Lithium and Alumina Extraction Efficiency

The effects of caustic concentration (K_2O) on lithium and alumina extraction rates are shown in Figure 4, which demonstrates that caustic concentration has a significant influence on the leaching process. Caustic concentration can promote the leaching of lithium and alumina from bauxite when $\rho(K_2O)$ is less than 250 g/L. When $\rho(K_2O)$ is higher than 250 g/L, the lithium extraction efficiency slightly slows down; therefore, the suitable caustic concentration is 250 g/L.

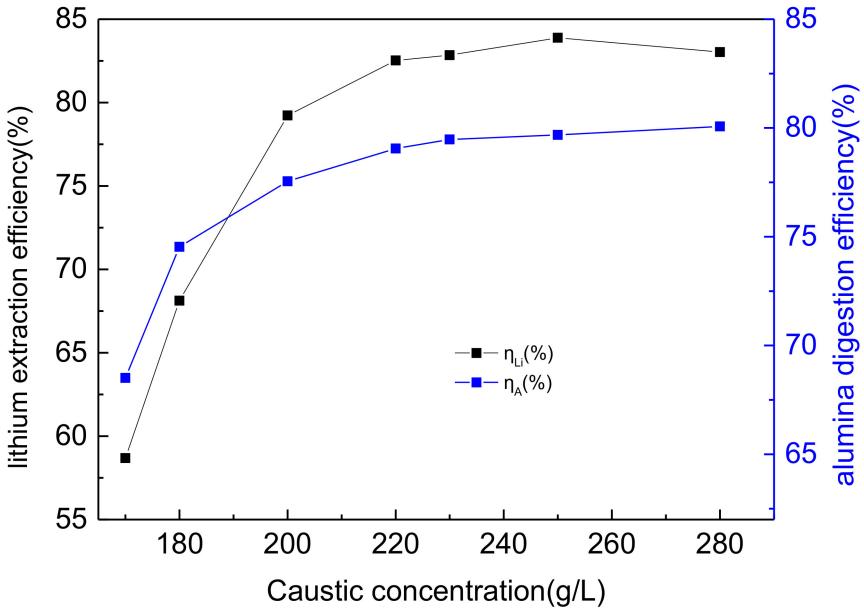

Figure 4. Effect of caustic concentration on lithium and alumina digestion behavior of bauxite (conditions: T = 265 °C, mass ratio of CaO/ore = 8%, t = 1 h).

Diaspore digestion reaction takes place on the interface between mineral and alkali solution, which belongs to the control stage of surface chemical reaction [23]. Elevated K_2O concentration can increase alumina equilibrium concentration, which will promote

bauxite dissolution. Elevated K_2O promotes the process of reaction (5), but excessive K_2O will increase the viscosity of the system and affect the diffusion process of lithium dissolution [24]. No characteristic peak of cookeite can be found in Figure 5, demonstrating that lithium chlorite reacted completely. Silicon-bearing minerals first react with alkali entering into the solution in the form of potassium silicate [25] and then react with sodium aluminate solution to form potassium silicate hydrate entering into red mud in the high-temperature digestion process of a K_2O-Al_2O_3-H_2O system.

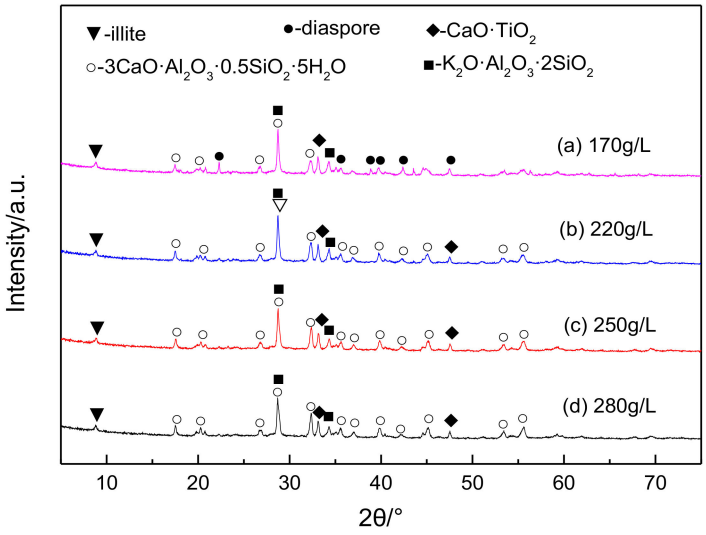

Figure 5. XRD patterns of red mud with different caustic concentrations (conditions: T = 265 °C, mass ratio of CaO/ore = 8%, t = 1 h).

3.3. The Effects of Temperature on Lithium and Alumina Extraction Efficiency

The digestion experiments were conducted at K_2O 254 g/L and a lime dosage of 8% for 60 min with different temperatures to explore the effects of digestion temperature on alumina and lithium extraction efficiencies; the results are shown in Figure 6.

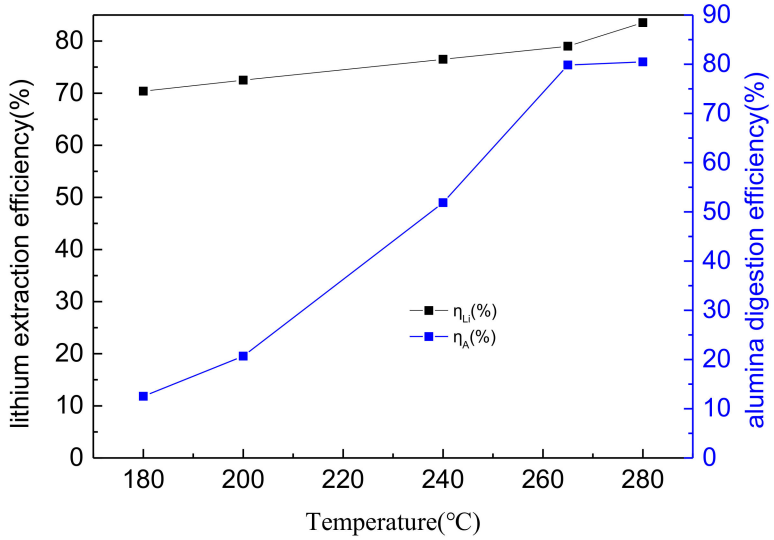

Figure 6. Effect of digestion temperature on lithium and alumina digestion behavior of bauxite (conditions: ρ (K_2O) = 254 g/L, mass ratio of CaO/ore = 8%, t = 1 h).

Figure 6 shows that digestion temperature has an obvious effect on the leaching process, which can promote the leaching of lithium and alumina from bauxite. The lithium extraction efficiency increases from 70.38% to 83.53% with temperature increasing from

180 to 280 °C. In contrast, the alumina extraction efficiency increases first and then tends to stabilize, arriving at a maximum value of 80.48% at 265 °C; therefore, the suitable digestion temperature is 265 °C. The XRD pattern (Figure 7) shows that no characteristic peak of cookeite can be found when the temperature is above 180 °C, demonstrating that cookeite reacted completely. In addition, there is the characteristic peak of diaspore when the temperature is below 265 °C, suggesting that the bauxite did not react completely. When the temperature is 280 °C, the characteristic peak of illite remains and does not change significantly, indicating that K_2O inhibits the dissolution reaction of illite with a high digestion temperature in a K_2O-Al_2O_3-H_2O system.

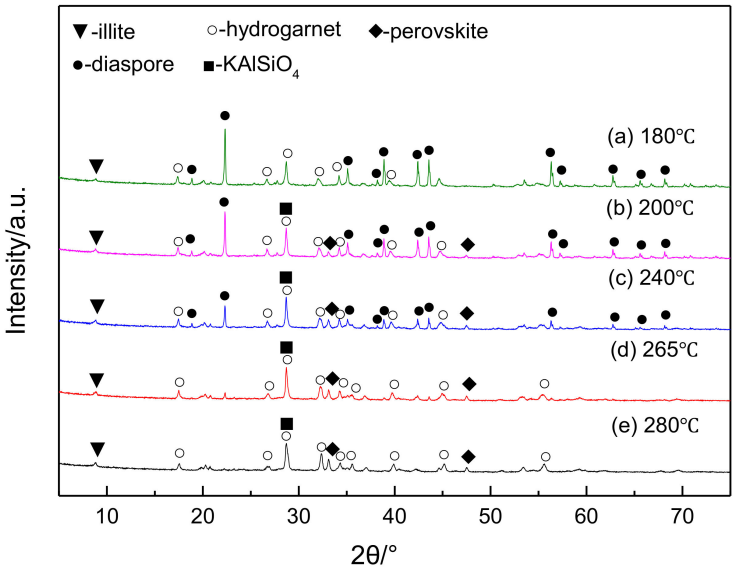

Figure 7. XRD patterns of red mud with different temperatures. (conditions: $\rho(K_2O)$ = 254 g/L, mass ratio of CaO/bauxite = 8%, t = 1 h).

3.4. The Effects of Duration on Lithium and Alumina Extraction Efficiency

The digestion experiments were conducted at K_2O254 g/L, 260 °C, and a lime dosage of 8% with different durations to explore the effects of reaction time on the alumina and lithium extraction rates; the results are shown in Figure 8.

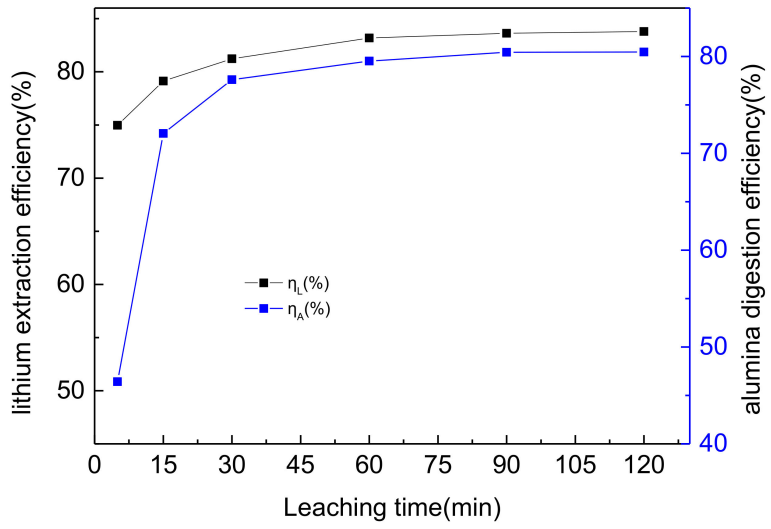

Figure 8. Effect of leaching time on lithium and alumina digestion of bauxite (conditions: $\rho(K_2O)$ = 254, mass ratio of CaO/ore = 8%, T = 265 °C).

As shown in Figure 8, the leaching time presents a remarkable effect on the lithium and alumina extraction efficiency. As leaching time increases from 5 min to 60 min, the lithium extraction efficiency increases from 74.97% to 83.18%, while the alumina extraction efficiency increases from 46.42% to 79.53%. However, further increasing the leaching time does not result in a clear increase in lithium and alumina. As shown in Figure 9, no characteristic peaks of cookeite were found, indicating that the reaction of cookeite was thorough. The diffraction peaks of diaspore still existed after increasing the leaching time to 30 min, but they were weaker. The diffraction peaks of diaspore disappeared when reacted for 60 min, the mineral decomposition was complete, and, thus, the suitable duration is 60 min.

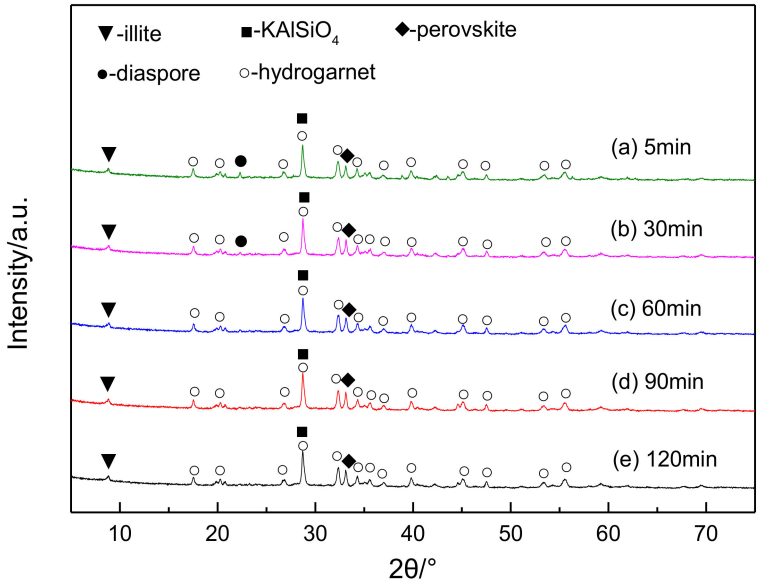

Figure 9. XRD patterns of red mud with different digestion times (conditions: $\rho(K_2O)$ = 254 g/L, mass ratio of CaO/ore = 8%, T = 265 °C).

3.5. Orthogonal Experiment

As shown in Section 3.4, when the duration is greater than 60 min, its effect is very small, and it is generally 60 min in real production. In order to clear the interactions among different impacts, orthogonal experiments were designed, where lime dosage, caustic concentration, and temperature were selected as variables. According to the design principles of the orthogonal experiment, an $L_9(3^4)$ orthogonal table was adopted, and each factor identified three levels (Table 4).

Table 4. Design of $L_9(3^4)$ orthogonal table.

NO.	Lime Dosage (%)	Temperature (°C)	K2O (g/L)
1	0	240	200
2	0	260	240
3	0	280	280
4	8	240	240
5	8	260	280
6	8	280	200
7	16	240	280
8	16	260	200
9	16	280	240

Tests were conducted according to the above designed experiment matrix in Table 4. During the date analysis process, η_L was selected as the objective function, and the results are shown in Table 5.

Table 5. Experimental scheme and analysis results based on η_L.

NO.	A	B	C	η_L (%)	η_A (%)
1	1	1	1	70.00	31.46
2	1	2	2	69.95	70.28
3	1	3	3	75.40	81.00
4	2	1	2	79.48	70.29
5	2	2	3	83.34	79.08
6	2	3	1	66.83	78.08
7	3	1	3	83.89	71.55
8	3	2	1	85.26	73.90
9	3	3	2	86.34	76.61

Based on the signal-noise ratio (SNR) and mean corresponding analysis, the order of each factor from primary to secondary is A (lime addition), C (K_2O, g/L), and B (temperature, °C). The best scheme is A3C3B2.

Based on the result of orthogonal experiments, the verified experiment was conducted at a caustic content of 280 g/L and at 260 °C with a lime dosage of 16% for 60 min. η_L and η_A are 85.6% and 80.09%, respectively, verified in accordance with the results of the orthogonal test.

4. Behavior Mechanism of Lithium during Digestion Process

The XRD pattern for red mud under the optimum leaching condition of a 16% lime dosage, a potassium concentration of 280 g/L, leaching temperature of 260 °C, and leaching duration of 60 minis shown in Figure 10, in which the main phase compositions are illite, hydrogarnet, perovskite, and $KAlSiO_4$. There is no characteristic peak of lithium chlorite and diaspore under this condition, which indicates that cookeite and diaspore reacted completely. Moreover, lithium and most alumina were extracted to the sodium aluminate solution.

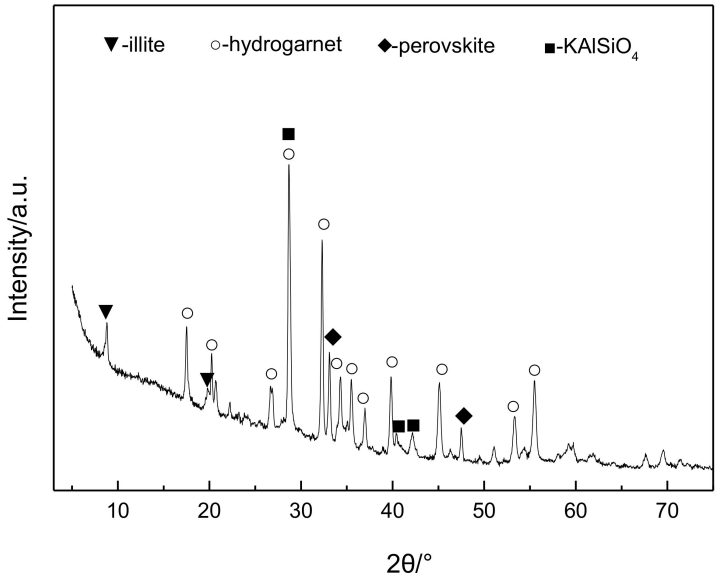

Figure 10. XRD patterns of red mud under the optimum condition($\rho(K_2O)$ = 280 g/L, mass ratio of CaO/ore = 16%, T = 260 °C).

Figures 11 and 12 shows the SEM images of lithium-bearing diaspore before and after digestion under optimal conditions, and Figure 12 confirms that the structure of the lithium-bearing diaspore is disrupted during leaching. As can be observed in Figure 12, the red mud is smaller in size than the bauxite (Figure 11.), and the structure has changed significantly, from crystallized slabs to dispersed flakes.

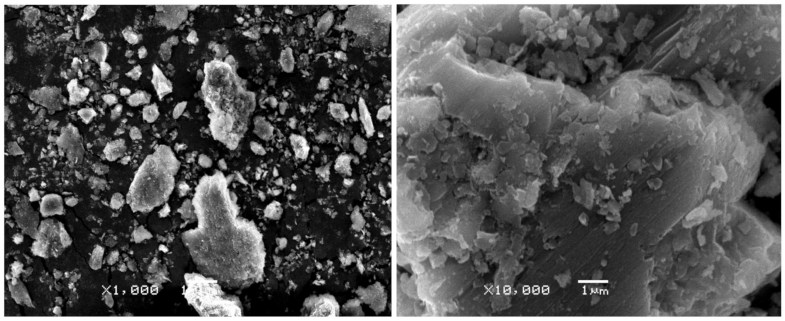

Figure 11. SEM image of Henan lithium-bearing diaspore.

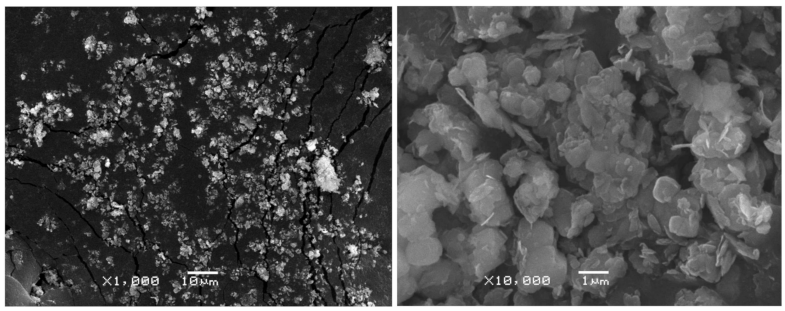

Figure 12. SEM image of red mud.

The cookeite is a layer of aluminum silicate minerals [26]. Strong chemical bonds exist between silica and alumina. Thus, high-temperature and high-pressure high alkali concentration in ambient conditions should be controlled, with which OH^- ions from the aluminum silicate crystals immersed inside the crystal surface, reacting with aluminum and silicon, making the aluminum silicate structure of osteoporosis [27].

From XRD results, it is speculated that the main reactions for the digestion of diaspore in K_2O-Al_2O_3-H_2O system can be expressed as follows:

$$2LiAl_4(Si_3Al)O_{10}(OH)_8) + 10KOH = 4KAl(OH)_4 + 2LiOH + 3K_2O{\cdot}Al_2O_3{\cdot}2SiO_2 + 4H_2O \quad (3)$$

$$2LiAl_4(Si_3Al)O_{10}(OH)_8) + 9KOH = 3KAl(OH)_4 + LiOH + LiAl(OH)_4 + 3K_2O{\cdot}Al_2O_3{\cdot}2SiO_2 + 4H_2O \quad (4)$$

$$2LiAl_4(Si_3Al)O_{10}(OH)_8) + 8KOH = 2KAl(OH)_4 + 2LiAl(OH)_4 + 3K_2O{\cdot}Al_2O_3{\cdot}2SiO_2 + 4H_2O \quad (5)$$

$$LiAl_4(Si_3Al)O_{10}(OH)_8 + 18Ca(OH)_2 + 7KAl(OH)_4 = 6(3CaO{\cdot}A1_2O_3{\cdot}0.5SiO_2{\cdot}5H_2O) + 7KOH + LiOH + 2H_2O \quad (6)$$

$$2LiAl(OH)_4 + K_2SiO_2(OH)_2 = Li_2SiO_3 + 2KAl(OH)_4 + H_2O \quad (7)$$

$$4LiOH + 2KAl(OH)_4 + 3K_2SiO_2(OH)_2 = 2LiAlSiO_4 + 8KOH + Li_2SiO_3 + 5H_2O \quad (8)$$

5. Conclusions

The results demonstrate that the mass ratio of the added CaO to bauxite, the KOH concentration, and the digestion temperature had a significant effect on the lithium extraction efficiency. An L9(3^4) orthogonal experiment demonstrated that the order of each factor for lithium extraction from primary to secondary is lime dosage, caustic concentration, and reaction temperature. Under the optimal conditions (t = 60 min, T = 260 °C, $\rho(K_2O)$ = 280 g/L, and 16% lime dosage), the leaching efficiencies of lithium and alumina are 85.6% and 80.09%, respectively, with about 15% of lithium entering into red mud.

Author Contributions: Conceptualization, D.H and Z.P.; methodology, D.H. and Z.P.; validation, D.H.; formal analysis, D.H., Z.P and E.S.; investigation, D.H.; Z.P. and E.S.; resources, D.H., Z.P., E.S. and L.S.; data curation, D.H. and E.S.; writing—original draft preparation and writing—review and editing, D.H., Z.P., E.S. and L.S.; supervision, Z.P. All authors have read and agreed to the published version of the manuscript.

Funding: This research received no external funding.

Data Availability Statement: The data used to support the findings of this study are available from the corresponding author upon request.

Conflicts of Interest: The authors declare no conflict of interest.

References

1. Cao, A.; Li, C. Enrichment mechanism of lithium in Bayer process of alumina production. *Nonferrous Met. (Extr. Metall.)* **2017**, *9*, 23–26.
2. Li, C.; Huang, J. The existing state of lithium in the process of alumina production. *Light Met.* **2005**, *6*, 17–19. (In Chinese)
3. Wang, D.; Li, P.; Qu, W.; Yin, L.; Zhao, Z.; Lei, Z.; Wen, S. Discovery and preliminary study of the high tungsten and lithium contents in the Dazhuyuan bauxite deposit, Guizhou, China. *Sci. China (Earth Sci.)* **2013**, *56*, 145–152. (In Chinese) [CrossRef]
4. Qing-Tao, H.U.; Liang, Y.D.; Wang, C.Z.; Xu-Jian, W.U.; Zhou, C.Q.; Niu, T.T. Effect of high lithium electrolyte on aluminum electrolysis production and improvement measures. *Nonferrous Met. (Extr. Metall.)* **2018**, *43*, 34–38. (In Chinese)
5. Huang, W.; Liu, G.; Liu, P.; Qi, T.-G.; Li, X.-B.; Peng, Z.-H.; Zhou, Q.-S. Equilibrium concentration of lithium ion in sodium aluminate solution. *J. Cent. South Univ.* **2019**, *26*, 304–311. [CrossRef]
6. Lv, X.J.; Shuang, Y.J.; Jie, L. Physicochemical Properties of Industrial Aluminum Electrolytes Enriching Li and K: The liquidus temperature. *Metall. Mater. Trans. B* **2017**, *48*, 1315–1320. [CrossRef]
7. Saitov, A.V.; Bazhin, V.Y.; Povarov, V.G. On the application of lithium additives in the electrolytic production of primary aluminum. *Russ. Metall. (Metall.)* **2017**, *12*, 1018–1024. [CrossRef]
8. Morishige, T.; Haarberg, G.M.; Gudbrandsen, H.; Skybakmoen, E.; Solheim, A.; Takenaka, T. Effects of composition and temperature on current efficiency for aluminum electrolysis from cryolite-based molten alumina electrolytes. *ECS Trans.* **2017**, *77*, 997–1002. [CrossRef]
9. Chen, F. Effect of lithium and potassium salts on the production of prebaked cell. *J. Mater. Metall.* **2010**, *9*, 148–149.
10. Huang, W.; Liu, G.; Ju, J.; Li, X.; Zhou, Q.; Qi, T.; Peng, Z. Effect of lithium ion on seed precipitation from sodium aluminate solution. *Trans. Nonferrous Met. Soc. China* **2019**, *29*, 1323–1331. [CrossRef]
11. Prestidge, C.A.; Ametov, I. Cation effects during aggregation and agglomeration of gibbsite particles under synthetic Bayer crystallization conditions. *J. Cryst. Growth* **2000**, *209*, 924–933. [CrossRef]
12. Van Straten, H.A.; Schoonen, M.A.A.; De Bruyn, P.L. Precipitation from supersaturated aluminate solutions. III. Influence of alkali ions with special reference to Li^+. *J. Colloid Interface Sci.* **1985**, *103*, 493–507. [CrossRef]
13. Xu, X.; Zhou, Y.; Fan, M.; Lv, Z.; Tang, Y.; Sun, Y.; Chen, Y.; Wan, P. Lithium adsorption performance of a three-dimensional porous H_2TiO_3-type lithium ion-sieve in strong alkaline Bayer liquor. *RSC Adv.* **2017**, *7*, 18883–18891. [CrossRef]
14. Tang, W.; Peng, Z.; Liu, G.; Zhou, Q.; Qi, T.; Li, X. Lithium removal from sodium aluminate solution and its reaction mechanism. *J. Cent. South Univ. (Sci. Technol.)* **2020**, *51*, 19–26.
15. Yin, Z. Research on the Behavior of Diasporic Bauxite in the Bayer Preheating and Digestion Process. Ph.D. Thesis, Northeastern University, Shenyang, China, 2005. (In Chinese)
16. Gu, S.; Yin, Z.; Zhou, H. Behavior of illite in the Bayer digestion process of diasporic bauxite. *Light Met.* **1992**, 109–112.
17. Yin, Z.; Gu, S.; Huang, H. The influence of K_2O in spent liquor on Bayer process of diasporic bauxite. *Light Met.* **2003**, 173–176.
18. Power, G.; Gräfe, M.; Klauber, C. Bauxite residue issues: I. Current management, disposal and storage practices. *Hydrometallurgy* **2011**, *108*, 33–45. [CrossRef]
19. Ma, S.H.; Wen, Z.G.; Chen, J.N.; Zheng, S.L. An environmentally friendly design for low-grade diasporic-bauxite processing. *Miner. Eng.* **2009**, *22*, 793–798. [CrossRef]
20. Malts, N.S. Efficiency of lime use in Bayer alumina production. *Light Met.* **1992**, 1337–1342.
21. Smith, P. Reactions of lime under high temperature Bayer digestion conditions. *Hydrometaurgy* **2017**, *170*, 16–23. [CrossRef]
22. Wang, Y.; Zhang, T.A.; Lv, G.; Zhang, W.; Zhu, X.; Xie, L. Reaction behaviors and amorphization effects of titanate species in pure substance systems relating to Bayer digestion. *Hydrometallurgy* **2017**, *171*, 86–94. [CrossRef]
23. Bi, S. *Alumina Production Process*; Chemical Industry Press: Beijing, China, 2010; pp. 8–9.
24. Wu, H.F.; Chen, C.Y.; Li, J.Q.; Lan, Y.P.; Wang, L.Z.; Quan, B.L.; Jin, H.X. Digestion mechanism and crystal simulation of roasted low-grade high-sulfur bauxite. *Trans. Nonferrous Met. Soc. China* **2020**, *30*, 1662–1673. [CrossRef]
25. Ma, Q.X.; Zhang, Y.F.; Cao, S.T.; Zhang, Y. Leaching behavior of diaspore bauxite in KOH sub-molten salt. *Chin. J. Process Eng.* **2013**, *13*, 391–396. (In Chinese)
26. Zheng, H.; Bailey, S.W. Refinement of the cookeite "r" structure. *Am. Mineral.* **1997**, *82*, 1007–1013. [CrossRef]
27. Zhao, H.; Hu, C.; Ma, H.; Wang, L.; Li, J.; Liu, Y. Digestion of potassium feldspar ore through high pressure hydrochemical process. *China's Manganese Ind.* **2002**, *20*, 27–29, (In Chinese with English Abstract)